This article was downloaded by:
On: *25 January 2011*
Access details: *Access Details: Free Access*
Publisher *Taylor & Francis*
Informa Ltd Registered in England and Wales Registered Number: 1072954 Registered office: Mortimer House, 37-41 Mortimer Street, London W1T 3JH, UK

Liquid Crystals
Publication details, including instructions for authors and subscription information:
http://www.informaworld.com/smpp/title~content=t713926090

A statistical study for evolving arrays of nematic point defects

P. Biscari; G. Guidone Peroli; E. G. Virga

Online publication date: 06 August 2010

To cite this Article Biscari, P. , Peroli, G. Guidone and Virga, E. G.(1999) 'A statistical study for evolving arrays of nematic point defects', Liquid Crystals, 26: 12, 1825 — 1832
To link to this Article: DOI: 10.1080/026782999203463
URL: http://dx.doi.org/10.1080/026782999203463

PLEASE SCROLL DOWN FOR ARTICLE

Full terms and conditions of use: http://www.informaworld.com/terms-and-conditions-of-access.pdf

This article may be used for research, teaching and private study purposes. Any substantial or systematic reproduction, re-distribution, re-selling, loan or sub-licensing, systematic supply or distribution in any form to anyone is expressly forbidden.

The publisher does not give any warranty express or implied or make any representation that the contents will be complete or accurate or up to date. The accuracy of any instructions, formulae and drug doses should be independently verified with primary sources. The publisher shall not be liable for any loss, actions, claims, proceedings, demand or costs or damages whatsoever or howsoever caused arising directly or indirectly in connection with or arising out of the use of this material.

LIQUID CRYSTALS, 1999, VOL. 26, NO. 12, 1825–1832

A statistical study for evolving arrays of nematic point defects

P. BISCARI*

Dipartimento di Matematica, Politecnico di Milano, via Bonardi 9, 20133 Milano, Italy; Istituto Nazionale di Fisica della Materia, 27100 Pavia, Italy

G. GUIDONE PEROLI and E. G. VIRGA

Dipartimento di Matematica, Università di Pavia, Istituto Nazionale di Fisica della Materia, via Ferrata 1, 27100 Pavia, Italy

(*Received 12 April 1999; accepted 8 August 1999*)

We study the dynamics of nematic point defects within a capillary tube enforcing homeotropic anchoring on the lateral boundary. At the initial time a great many of them, with topological charges alternating in sign, may be created at random along the axis of the cylinder; they then evolve, subject to their mutual interactions, and eventually reach an equilibrium configuration, possibly after having suffered many annihilations. Here we see how the arrays of surviving defects depend on both the length of the tube and the number of initial defects. We arrive at the equilibrium distribution of the distance between defects by solving the appropriate evolution equations over many simulations. The information we thus obtain on the average spacing could be tested experimentally.

Downloaded At: 18:59 25 January 2011

1. Introduction

In 1970 Dzyaloshinskiĭ [1] predicted that a nematic liquid crystal confined to a cylindrical tube which enforces homeotropic anchoring on its lateral boundary could only exhibit a splay deformation of the director **n**, which would thus take on a radial configuration with a line disclination along the axis. However, Cladis and Kleman [2], as well as Meyer [3], proved that there is another configuration for **n**, which for cylinders with diameter larger than 0.1 μm would indeed store less energy than the radial one: this is the *escaped* field, where **n** is continuous throughout the cylinder and exhibits a bend deformation as it flips out of the plane orthogonal to the axis. Actually, there are two such fields: one escapes upwards and the other downwards; they can be transformed into one another by a reflection through a plane orthogonal to the axis, and so they store the same energy density. Optical observations confirmed the existence of these escaped configurations, but they also revealed the presence of arrays of point *defects*; that is, discontinuities in the director field sitting on the axis of the tube. A defect appears wherever the opposite escaped fields come together, and so in an array, the topological charge, which bears information on the director field around each defect, alternates in sign.

*Author for correspondence.

Arrays of defects give rise to interesting co-operative phenomena which have been observed in cylinders with radius R in the range 2–3 μm [4] and, more recently, even in cylinders with radius well below a micron [5–7]. These latter observations were performed with the aid of deuterium-nuclear-magnetic resonance, and the average spacing in the arrays was determined by comparing the experimental spectra and those obtained by either simulating numerically the director field or employing a trial function to describe it.

It has long been known that when two defects with opposite topological charges are sufficiently close to one another, they attract each other, coalesce, and finally annihilate leaving no trace behind. On the other hand, when two defects are sufficiently far away, they do not move, and behave as if the interaction force between them were screened. A theoretical model for the interaction between two defects is developed in [8]; it estimates the *critical distance* d_c, above which the interaction ceases, as $d_c \simeq 2.2R$. Within an array the interactions between defects are more involved, since in general one defect *feels* the presence of two others from opposite sides: an array becomes stable only when every defect is screened from the two adjacent defects, possibly after many annihilations have taken place. Here we aim at describing for a large number of defects the dynamical evolution leading to stable arrays.

Journal of Liquid Crystals ISSN 0267-8292 print/ISSN 1366-5855 online © 1999 Taylor & Francis Ltd
http://www.tandf.co.uk/JNLS/lct.htm
http://www.taylorandfrancis.com/JNLS/lct.htm

We extend the model introduced in [8] and [9] to account for a general system with N defects, writing both the elastic free energy and the dissipation function for a system with an arbitrary number of defects. Within this mathematical setting, we perform a statistical analysis to answer the following questions. Starting from a given number of defects, how many of them are likely to survive at the end? How does this number increase if more defects are present at the beginning? Does the number of surviving defects depend on the length of the tube? How are the surviving defects distributed along the axis?

The plan of the paper is the following. In §2 we derive the differential equations that govern the dynamics of the array. Section 3 is devoted to the analysis of the results of the numerical simulations based on these equations, which are then discussed in §4. Finally, in the Appendix, we show how to compute within our model the dissipation of the viscous torques acting on the director field for a system with an arbitrary number of defects.

Downloaded At: 18:59 25 January 2011

2. Dynamical system

Here we assume that the motion of the defects along the axis of a capillary tube enforcing homeotropic anchoring on the lateral boundary is due only to the rearrangement of the director field and that this does not entrain any hydrodynamic motion of the fluid: in other words, the *back-flow* is completely neglected. The equations of nemato-dynamics have recently been rederived by Leslie in [10] from a dissipation principle which, in the absence of back-flow, states that the energy $\mathscr{D}$ dissipated in the motion must balance the time derivative of the elastic free energy $\mathscr{F}$:

$$\dot{\mathscr{F}} + \mathscr{D} = 0. \tag{1}$$

No account is taken in (1) of any kinetic energy: no hydrodynamic motion is indeed present, whereas the director motion, though present, has negligible inertia.

Let $\mathscr{B}$ be the region in space occupied by the liquid crystal. The elastic free energy can be given the form

$$\mathscr{F}[\mathbf{n}] = \frac{K}{2}\int_{\mathscr{B}} |\nabla \mathbf{n}|^2 \, \mathrm{d}v, \quad \text{with } K > 0,$$

which is the *one-constant approximation* to Frank's free-energy functional [11]. In the absence of back-flow, $\mathscr{D}$ reduces to

$$\mathscr{D} = \gamma_1 \int_{\mathscr{B}} \left(\frac{\partial \mathbf{n}}{\partial t}\right)^2 \mathrm{d}v,$$

where $\gamma_1 > 0$ is the *rotational viscosity* (cf. e.g. Section 5.1.4.3 of [12]).

In [13] a model for the dynamics of a cluster of defects was built on the premiss that $\mathscr{F}$ is the potential energy of the system and $\mathscr{D}/2$ its Rayleigh's dissipation function. The equations of motion of this dynamical system can be derived in the classical form, with the only omission the kinetic terms, provided that $\mathscr{F}$ is given as a function of the Lagrangian coordinates of the defects and $\mathscr{D}$ as a function of these coordinates and their time derivatives (cf. e.g. p. 231 of [14]). These functions were obtained by resorting to an approximate description of $\mathbf{n}$ around a defect of either sign, which involves only a finite number of parameters. This method is explained in detail in [15] and need not be repeated here. Thus, defects become similar to particles, for which it suffices to assign the appropriate functions $\mathscr{F}$ and $\mathscr{D}$.

The model developed to describe the director field around a point defect has been employed in [9] and [13] to study the evolution of a system with five defects alternating in charge: an analytical study is performed there, along the lines of thought described above. Here we consider N defects with alternating charges moving along the axis of a cylinder with length L. To identify the positions of the defects in the system we use the following coordinates: ξ, which is the co-ordinate along the axis of the upper defect scaled to the radius R of the tube, and

$$\rho_i := \frac{d_i}{2\sqrt{\alpha\pi}\,R} \quad \text{for } i = 1, \ldots, N-1,$$

where $\alpha := 2\ln 2 - 1$, and d_i denotes the distance between the i-th defect and the $(i+1)$-th, the *first* defect being the upper one.

In our model, two defects interact as long as the distance between them does not exceed $d_c := 2\sqrt{\alpha\pi}\,R \simeq 2.2R$, and so the defects with labels i and $(i+1)$ interact as long as their scaled distance ρ_i does not exceed 1. The reason is that the distortion in the director field around a point defect has a finite length, which is precisely $\sqrt{\alpha\pi}R$: farther away, the escaped configurations prevail. Thus, when the distance between two defects with opposite topological charges is larger than d_c, bringing them closer to one another would formally amount to displacing regions with one escaped field into regions with the other one. Clearly, no change in the elastic free energy is involved in this exchange, since both escaped fields store the same energy density: the defects freely fluctuate in the tube, each unaware of the presence of the other. A detailed explanation for this can be found in [8].

As illustrated in detail in the Appendix, it can be proved by mathematical induction that the elastic free energy and the dissipation have the following forms in terms of the coordinates of the system:

$$\mathscr{F}_N(\rho) := 2\pi K R \sqrt{\alpha\pi} \sum_{i=1}^{N-1} (1 - \ln \rho_i)\rho_i \tag{2}$$

and

$$\mathscr{D}_N(\xi, \rho, \dot{\xi}, \dot{\rho}) := 2\pi\gamma_1 \alpha R^3 \left\{ \sqrt{\frac{\pi}{\alpha}} \left(1 + \sum_{i=1}^{N-1} \rho_i\right) \dot{\xi}^2 + 2\pi \sqrt{\alpha\pi} \left[\sum_{k=1}^{N-1} \left(\beta\rho_k + 2 \sum_{i=k+1}^{N-1} \rho_i + 1\right) \dot{\rho}_k^2 + \sum_{i<j} \left(2\rho_j + 4 \sum_{k>j} \rho_k + 2\right) \dot{\rho}_i \dot{\rho}_j \right] - 2\pi\dot{\xi} \sum_{k=1}^{N-1} \left(\rho_k + 2 \sum_{i=k+1}^{N-1} \rho_i + 1\right) \dot{\rho}_k \right\}$$

where $\rho := (\rho_1, \dots, \rho_{N-1})$ and $\dot{\rho} := (\dot{\rho}_1, \dots, \dot{\rho}_{N-1})$. The equations of motion for this system are

$$\begin{cases} \dfrac{\partial \mathscr{F}_N}{\partial \xi} + \dfrac{1}{2} \dfrac{\partial \mathscr{D}_N}{\partial \dot{\xi}} = 0 \\ \dfrac{\partial \mathscr{F}_N}{\partial \rho_i} + \dfrac{1}{2} \dfrac{\partial \mathscr{D}_N}{\partial \dot{\rho}_i} = 0 \quad \text{for } i = 1, \dots, N-1. \end{cases} \tag{4}$$

It should be noted that the dissipation principle in (1) is identically satisfied along all solutions of equations (4), since $\mathscr{D}_N$ is quadratic in the variables $(\dot{\xi}, \dot{\rho})$. From (2) and (3), the differential equations in (4) become

$$\begin{cases} \dot{\xi} = \dfrac{\sqrt{\alpha\pi}}{1 + \sum_{i=1}^{N-1} \rho_i} \left[\sum_{i=1}^{N-1} \left(1 + \rho_i + 2 \sum_{k=i+1}^{N-1} \rho_k\right) \dot{\rho}_i \right] \\ \dfrac{1}{T} \ln \rho = \boldsymbol{A} \dot{\rho} \end{cases} \tag{5}$$

where $T := \alpha\pi\gamma_1 R^2 / K$ is a relaxation time, and the entries of the matrix $\boldsymbol{A}$ are defined by

$$\boldsymbol{A}_{ii} := 2\left(\beta\rho_i + 2 \sum_{j=i+1}^{N-1} \rho_j + 1\right) - \frac{\left(1 + \rho_i + 2 \sum_{j=i+1}^{N-1} \rho_j\right)^2}{\sum_{j=1}^{N-1} \rho_j + 1}$$

$$\boldsymbol{A}_{ki} := 2\left(\rho_i + 2 \sum_{j=i+1}^{N-1} \rho_j + 1\right) - \frac{\left(1 + \rho_k + 2 \sum_{j=k+1}^{N-1} \rho_j\right)\left(1 + \rho_i + 2 \sum_{j=i+1}^{N-1} \rho_j\right)}{\sum_{j=1}^{N-1} \rho_j + 1} \quad \text{for } k < i$$

$$\boldsymbol{A}_{ki} := \boldsymbol{A}_{ik} \quad \text{for } k > i$$

where both i and k range in $\{1, \dots, N-1\}$. In the following section equations (5) are studied numerically.

3. Surviving defects

Here we describe the outcomes of numerical simulations performed on several different systems of interacting defects, by varying both the length of the cylinder and the number of initial defects. We considered cylinders with radius R and length L equal to 10, 25, 50, and 100 times the critical distance $d_c = 2\sqrt{\alpha\pi}\, R$, above which two defects become independent from one another. Thus, for example, when $L = nd_c$, the maximum number of defects that can be packed at equilibrium is precisely $n+1$: this maximum packing can be obtained only in the configuration where the first defect is placed just on one base of the cylinder, and all others are equally spaced at the distance d_c.

For every prescribed value of L, we also varied the number N_i of initial defects: for each choice of L and N_i, we performed 50 000 simulations to obtain significant averages on both the number of surviving defects and their distribution along the axis. The defects were initially placed at random along the axis, and then allowed to evolve according to the differential equations of motion (5). Clearly, during the evolution the whole array splits into sub-arrays of interacting defects, to which equations (5) are to be applied separately. In particular, when a sub-array consists of just two defects separated by a distance less than d_c, their interaction always results in an annihilation. Since the arrays are always constituted by defects with alternating charges, all interactions are attractive, and the evolution always leads every single sub-array to a global contraction, with both head and tail, as it were, pushed inwards. This property implies that every time the distance between two adjacent defects grows up to the critical value d_c, the sub-array to which they belong breaks into two others, which will never interact again with one another.

3.1. *Density of surviving defects*

For given L and N_i, we call N_f the total number of defects in the final configuration, which does not further evolve because all surviving defects are farther apart than d_c, so that they feel no force. To represent the data, it is expedient to define the *densities*

$$n_i := \frac{N_i - 1}{L} d_c, \qquad n_f := \frac{N_f - 1}{L} d_c.$$

They are, respectively, the numbers of initial and surviving defects to be found on average over the critical distance. Figure 1 shows how the density of surviving defects n_f depends on both the density of initial defects n_i and the length of the cylinder L. Every point in the figure corresponds to an average over 50 000 simulations all made for the same values of L and N_i. Several remarks are needed to understand better the results shown in this figure.

Downloaded At: 18:59 25 January 2011

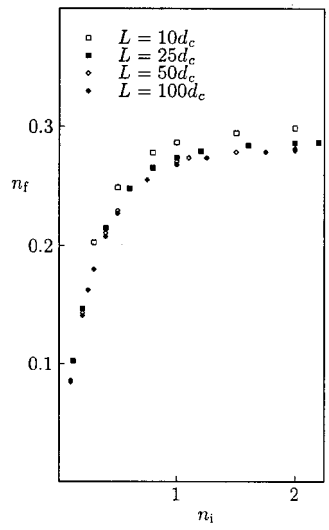

Figure 1. The density n_f of surviving defects as a function of the density n_i of initial defects.

(1) For each prescribed length of the cylinder, as long as the defects are created at random along the axis, as is always the case in our simulations, there is a maximum number of defects that may survive in the cylinder. If we recall that the theoretical limit on $(N_f - 1)$ is L/d_c, so that n_f cannot exceed 1, it is quite a surprise to discover that on average less than 30% of the maximum number of allowed defects survive in the cylinder. This result also allows us to estimate the average distance between defects in the final equilibrium configurations, which is formally defined as

$$d_f := \frac{L}{\langle N_f \rangle - 1}$$

where $\langle N_f \rangle$ is the average of N_f over all simulations with given L and N_i. Figure 1 shows that for $n_i > 1$ the average distance d_f ranges from $3d_c$ to $4d_c$. Finally, recalling that $d_c \simeq 2.2R$, we arrive at the following estimate:

$$d_f = 8R \pm 2R. \tag{6}$$

(2) For every fixed value of L, the density n_f of surviving defects reaches a *plateau* when n_i approaches 1, that is, when $(N_i - 1)$ approaches L/d_c: further packing of initial defects gives only a negligible increase in the number of surviving defects.

(3) The density n_f decreases for longer cylinders. This effect can be explained as follows. Consider, for example, a cylinder with length L, and compare the number of defects surviving in it with the sum of those surviving in two cylinders with length $L/2$. There are equilibrium configurations in the pair of shorter cylinders that lead to further annihilations, when seen as configurations for the longer cylinder, since a pair of defects closer than d_c, one in each half-cylinder, tend to annihilate in the whole cylinder.

3.2. *Random packing model*

The results of our simulations can also be predicted quite accurately by the following naïve model, which will be referred to as the *Random Packing Model*. Suppose we try to pack N_i defects on the axis of a cylinder with length L. We begin by placing at random the first defect. Then, we lay the second defect: if the two defects happen to lie at a distance smaller than d_c, we assume they will annihilate, and so we simply delete them. Later, we place the third defect, and we check again whether it annihilates with one of the first two defects, if they are still present. Thus, at each stage we put a defect at random on the axis and, if the defect nearest to it falls at a distance smaller than d_c, we annihilate both. After N_i attempts, we simply count the numbers of surviving defects. Figure 2 shows a comparison between the outcomes of both the analytic simulation and the Random Packing Model obtained for $L = 10d_c$ and $L = 100d_c$. Here the continuous line also comes from averages over 50 000 different attempts for each value of L and N_i.

The results obtained with the Random Packing Model are clearly more accurate when N_i is small, since the main difference between the two models is that the analytic simulation takes into account the interactions between all defects belonging to the same sub-array, while the Random Packing Model only considers pair interactions: large sub-arrays, however, are not probable when N_i is small. In any case, the predictions also remain quite accurate when N_i increases and many defects

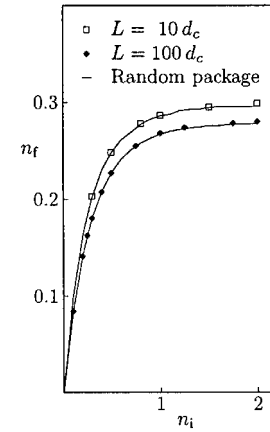

Figure 2. The density n_f of surviving defects as a function of the density n_i of initial defects, in both the analytic and Random Packing models.

Downloaded At: 18:59 25 January 2011

interact together. This fact indicates that the characteristic time for a single annihilation is sensibly smaller than the characteristic time of co-operative interactions.

3.3. *Distribution of defects*

Figure 3 explains how the surviving defects tend to be distributed along the axis of the cylinder. Let x be a coordinate on this axis and let $d_f(x)$ be the average over all final equilibrium configurations of the distance between the two defects with coordinates nearest to x. Thus, wherever $d_f(x)$ is sensibly smaller than d_f, the defects tend to remain closer to one another, though still at equilibrium. Clearly, the distance between two adjacent defects can never be smaller than d_c when the array reaches its equilibrium configuration. Here, all departures from a uniform distribution, which would be predicted by the Random Packing Model, are due to the co-operative interactions between defects. In figure 3, for every $0 \leqslant x \leqslant L$, the *local* average $d_f(x)$ is compared with d_f.

Figure 3 (*a*) represents the simulations made for cylinders with length $L = 10d_c$. It shows a curious oscillatory behaviour of the distribution $d_f(x)$: near the ends of the cylinders, almost at the distance d_c, $d_f(x)$ is 1% greater than its average value d_f. Then, at the distance $2d_c$ from the ends, $d_f(x)$ is close to its minimum value, which is 4% smaller than d_f. Finally, the maximum value of $d_f(x)$ falls in the middle of the cylinder. Thus, although all

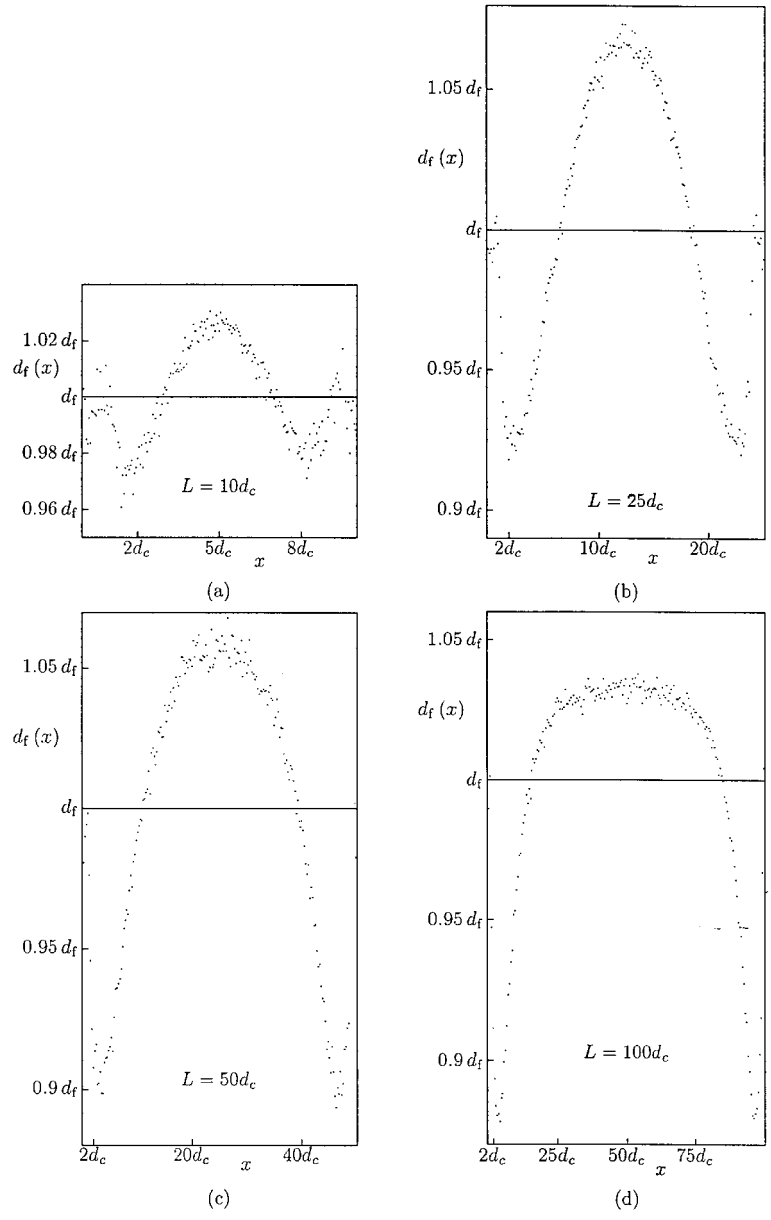

Figure 3. Distribution of the distance between defects along the axis of a cylinder with length $10d_c$ (*a*), $25d_c$ (*b*), $50d_c$ (*c*), and $100d_c$ (*d*).

Downloaded At: 18:59 25 January 2011

these effects are small, the defects prefer to be packed at a distance almost $2d_c$ from the ends.

Figure 3 (*b*) shows how the situation changes when the cylinder is longer ($L = 25d_c$). All the effects present in figure 3 (*a*) are here confirmed, and even magnified, since the minimum value of $d_f(x)$ is now 7% below the average value. The most interesting fact is that the minimum of d_f falls again at a distance almost $2d_c$ from the ends, thus indicating an *edge effect*, since this distance does not scale with L.

Figure 3 (*c*), which refers to a cylinder with $L = 50d_c$, confirms this trend: $d_f(x)$ still attains its minimum at a few d_c lengths from the ends, where it is now more than 10% below the average value d_f. On the other hand, there is no trace here of the relative maximum that $d_f(x)$ attains for shorter cylinders at a distance close to $1d_c$ from the ends.

Figure 3 (*d*) gives a clear idea of how defects tend to be distributed in cylinders with large aspect ratios (here $L/2R > 100$). The distribution $d_f(x)$ is almost uniform in the middle, as one would have expected. Moreover, an edge effect, extended over the length $10d_c$, tends to pack the defects closer to one another: the minimum distance between defects, which here is almost 15% smaller than d_f, is attained at a distance of a few d_c lengths from the ends.

Downloaded At: 18:59 25 January 2011

4. Discussion

We have extended the model first introduced in [9] to describe the motion and annihilation of nematic point defects distributed along the axis of a cylindrical tube. In [9] a system with only five initial defects was considered: they formed arrays with the distance between adjacent defects always less than d_c, so that from the start all defects participated in the motion. It was proved that in 81% of the cases only one defect survives at the end, while in the remaining 19% of cases three defects survive. A further analysis of this case showed that the average distance d_f in the surviving arrays with three defects is close to $2.9R$. This result can also be explained by a naïve argument. Since point defects always annihilate in pairs to keep constant the total topological charge of the system, only two cases can result from the evolution of five defects: either one or three defects survive. In the former case, there is no average distance to talk about. In the latter case, the distance beween two adjacent surviving defects must always range between d_c and $2d_c$, because an equilibrium configuration with three defects can only be obtained from the coalescence of the three inner defects into the one in the middle. Thus, d_f is expected to be close to $1.5d_c$, that is, $d_f \simeq 3R$.

To frame this result into the present analysis, we should also account for the other 81% cases, where a single defect survives. Thus, the initial array with five defects is to be thought of as if it were an independent sub-array of a larger one; that is, as if next to both the first and the last defect there were two peripheral defects, each at a distance greater than d_c. Therefore, in 81% of cases the average distance between the only surviving defect and the peripheral ones is at least $3d_c \simeq 6.6R$. From this argument we can roughly estimate the average distance d_f to be about $6R$. Here we have considered arrays of defects initially distributed at random along the axis of a cylinder with fixed length. In this case the array splits into indepenent sub-arrays that will never interact with one another, as each will tend to collapse towards its middle. Thus, the average distance d_f estimated above must be greater than the one computed in [9], since now we are also taking into account defects that were never closer than the critical distance d_c.

Actually, the whole probability distribution of the equilibrium distances between defects can be estimated with our method: figure 4 shows the results obtained from 500 000 runs made on a cylinder with length $L = 50R$. Half the runs were made with an initial number of defects $N_i = 25$, and half with $N_i = 26$, so that the effects due to the different cardinality of N_i would cancel. This graph clearly explains why the experimental studies [5–7] revealed an average distance between surviving defects close to $3R$: in fact, this is the most probable distance to arise in the final equilibrium configuration. Larger distances, of the order of $10R$ or higher, have a smaller probability to occur, but the average distance we have estimated in (6) clearly accounts for all of them: d_f is

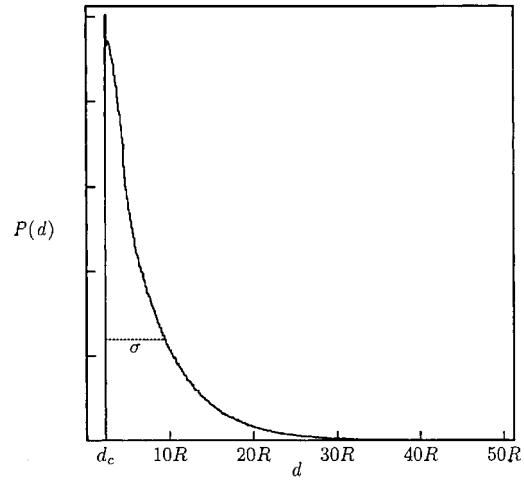

Figure 4. Probability distribution of the distance between defects. The maximum of the probability is attained near the critical distance $d = d_c$. This means that most of the defects remain at a distance $d \simeq 2.2R$ from one another. The variance of the distribution is $\sigma = 7.2R$. The data were obtained from 500 000 runs made on a cylinder with length $L = 50R$. The probability density $P(d)$ is expressed in arbitrary units.

approximately $8R$ because the probability distribution is highly non-symmetric. More detailed experiments could possibly reveal other features of the distribution of residual distances predicted by our model.

We gratefully acknowledge an enlightening discussion with G. Durand on the Random Packing Model. One of us (G.G.P.) also wishes to thank the Italian Istituto Nazionale di Alta Matematica for having supported her work.

Appendix

Proof by induction

Formula (3) can be given the following proof by induction. We know from [13] that for a system of three defects the dissipation is given by

$$\begin{aligned}\mathscr{D}_3(\dot{\xi},\dot{\rho}_1,\dot{\rho}_2) = 2\pi\gamma_1\alpha R^3\Big\{&\sqrt{\frac{\pi}{\alpha}}(1+\rho_1+\rho_2)\dot{\xi}^2\\ &+2\pi\sqrt{\alpha\pi}\big[(\beta\rho_1+2\rho_2+1)\dot{\rho}_1^2\\ &+(\beta\rho_2+1)\dot{\rho}_2^2+(2\rho_2+2)\dot{\rho}_1\dot{\rho}_2\big]\\ &-2\pi\dot{\xi}\big[(\rho_1+2\rho_2+1)\dot{\rho}_1+(\rho_2+1)\dot{\rho}_2\big]\Big\}\end{aligned} \tag{A1}$$

where, at variance with formula (3.23) in [13], we have set $\zeta_0 = \xi - 2\sqrt{\alpha\pi}\rho_1$ and exchanged the rôles of ρ_1 and ρ_2. Equation (A1) easily follows from (3) when $N=3$. Moreover, we now proceed to show that by use of (3) the dissipation of a system with $N+1$ defects can be expressed as

$$\begin{aligned}&\mathscr{D}_{N+1}(\xi,\rho,\dot{\xi},\dot{\rho})\\ &\quad= 2\pi\gamma_1\alpha R^3\Big\{\sqrt{\frac{\pi}{\alpha}}\Big(1+\sum_{i=1}^{N}\rho_i\Big)\dot{\xi}^2\\ &\qquad+2\pi\sqrt{\alpha\pi}\Big[\sum_{k=1}^{N}\Big(\beta\rho_k+2\sum_{i=k+1}^{N}\rho_i+1\Big)\dot{\rho}_k^2\\ &\qquad+\sum_{i<j<N}\Big(2\rho_j+4\sum_{N>k>j}\rho_k+2\Big)\dot{\rho}_i\dot{\rho}_j\Big]\\ &\qquad-2\pi\dot{\xi}\sum_{k=1}^{N}\Big(\rho_k+2\sum_{i=k+1}^{N}\rho_i+1\Big)\dot{\rho}_k\Big\}\end{aligned} \tag{A2}$$

where now $\rho := (\rho_1,\dots,\rho_N)$ and $\dot{\rho} := (\dot{\rho}_1,\dots,\dot{\rho}_N)$. In fact, when we add the $(N+1)$-th defect to a system with N defects, we modify the structure of the director field only near the N-th defect: this latter now interacts with the new one, and so the new parameter ρ_N must also be introduced. The contribution to the dissipation that in equation (3) comes from the region beyond the N-th defect is the same as the one which now comes from the region beyond the $(N+1)$-th defect, apart from renaming the parameters. In computing $\mathscr{D}_{N+1}$ this contribution can formally be accounted for by adding to $\mathscr{D}_N$ the quantity

$$\mathscr{D}_{N,N+1} := 2\pi\gamma_1\alpha R^3\Big(2\pi\sqrt{\alpha\pi}\dot{\rho}_N^2 - 2\pi\dot{\xi}\dot{\rho}_N + 4\pi\sqrt{\alpha\pi}\dot{\rho}_N\sum_{i<N}\dot{\rho}_i\Big).$$

Two further contributions come to the dissipation arising from the $(N+1)$-th defect: they can be computed as illustrated in [13], and together amount to

$$\begin{aligned}\mathscr{D}_{N+1,N} := 2\pi\gamma_1\alpha R^3\Big[&\sqrt{\frac{\pi}{\alpha}}\rho_N\dot{\xi}^2+4\pi\sqrt{\alpha\pi}\rho_N\Big(\sum_{i<N}\dot{\rho}_i\Big)^2\\ &+2\pi\sqrt{\alpha\pi}(1+\beta)\rho_N\dot{\rho}_N^2-4\pi\rho_N\dot{\xi}\sum_{i<N}\dot{\rho}_i\\ &-2\pi\dot{\xi}\rho_N\dot{\rho}_N+2\pi\sqrt{\alpha\pi}\rho_N\dot{\rho}_N\sum_{i<N}\dot{\rho}_i\Big].\end{aligned}$$

We thus arrive at

$$\begin{aligned}&\mathscr{D}_{N,N+1}+\mathscr{D}_{N+1,N}\\ &\quad=\sqrt{\frac{\alpha}{\pi}}\rho_N\dot{\xi}^2+2\pi\sqrt{\alpha\pi}\Big(\beta\dot{\rho}_N^2\rho_N+\dot{\rho}_N^2+2\rho_N\sum_{i<N}\dot{\rho}_i^2\Big)\\ &\qquad+2\pi\sqrt{\alpha\pi}\\ &\qquad\times\Big(2\rho_N\dot{\rho}_N\sum_{i<N}\dot{\rho}_i+4\rho_N\sum_{i<j<N}\dot{\rho}_i\dot{\rho}_j+2\dot{\rho}_N\sum_{i<N}\dot{\rho}_i\Big)\\ &\qquad-2\pi\dot{\xi}\Big(\rho_N\dot{\rho}_N+2\rho_N\sum_{i<N}\dot{\rho}_i+1\Big)\end{aligned}$$

which must be added on the right-hand side of equation (3) to give $\mathscr{D}_{N+1}$. One easily sees that this reproduces formula (A2), and so the proof by induction is complete.

References

[1] Dzyaloshinskiĭ, I. E., 1970, *Zh. Eksp. Teor. Fiz.*, **31,** 773 (Sov. Phys. JETP, **33** (1970), 773).
[2] Cladis, P. E., and Klèman, M., 1972, *J. Phys. (Paris)*, **33,** 591.
[3] Meyer, R. M., 1973, *Phil. Mag.*, **77,** 405.
[4] Kuzma, M., and Labes, M. M., 1983, *Mol. Cryst. liq. Cryst.*, **100,** 103.
[5] Crawford, G. P., Vilfan, M., Doane, J. W., and Vilfan, I., 1991, *Phys. Rev. A*, **43,** 835.

Downloaded At: 18:59 25 January 2011

[6] Crawford, G. P., Allender, D. W., Doane, J. W., Vilfan, M., and Vilfan, I., 1991, *Phys. Rev. A*, **44,** 2570.
[7] Crawford, G. P., Allender, D. W., and Doane, J. W., 1992, *Phys. Rev. A*, **45,** 8693.
[8] Guidone Peroli, G., and Virga, E. G., 1996, *Phys. Rev. E*, **54,** 5235.
[9] Guidone Peroli, G., and Virga, E. G., 1997, *Phys. Rev. E*, **56,** 1819.
[10] Leslie, F. M., 1992, *Continuum Mech. Thermodyn.*, **4,** 167.
[11] Frank, F. C., 1958, *Discuss. Faraday Soc.*, **25,** 19.
[12] De Gennes, P. G., and Prost, J., 1993, *The Physics of Liquid Crystals*, 2nd Edn (Oxford: Clarendon Press).
[13] Guidone Peroli, G., and Virga, E. G., 1998, *Physica D*, **111,** 356.
[14] Whittaker, E. T., 1989, *A Treatise on the Analytical Dynamics of Particles and Rigid Bodies*, 4th Edn (Cambridge: Cambridge University Press).
[15] Guidone Peroli, G., and Virga, E. G., 1997, *IMA J. appl. Math.*, **58,** 211.

Downloaded At: 18:59 25 January 2011